Comparison of the Physical and Functional Properties of the 48-Subunit Native Molecule and the 24- and 12-Subunit Dissociation Intermediates of *Limulus polyphemus* Hemocyanin†

Michael Brenowitz,* Celia Bonaventura, and Joseph Bonaventura

ABSTRACT: *Limulus* hemocyanin is a 48-subunit complex that is composed of eight immunochemically distinct subunits. Conditions were established that allowed for comparison of the structural and functional properties of the native molecule with those of its 24-subunit and 12-subunit dissociation products by analytical ultracentrifugation, functional analysis, stopped-flow light scattering, and circular dichroism spectroscopy. The 48-subunit complex was found to be specifically stabilized by calcium ions. When 48-subunit molecules at pH 7 were rapidly mixed with a pH 9 buffer containing a calcium chelator, the dissociation to monomers was complete within minutes. The rate is dependent upon the concentration and Ca^{2+} affinity of the chelator, consistent with the formation of a transient chelator–calcium ion–protein complex during the dissociation process. Dissociation to the level of 24-subunit molecules occurs much more slowly than does the dissociation of 24-subunit molecules to monomers. The dissociation to monomers, from 48-, 24-, or 12-subunit aggregates, is a highly cooperative process, and the corresponding reassembly reactions show appreciable hysteresis. In contrast, the reversible dimerization of dodecamers appears to be a rapidly equilibrating system. The varied aggregation states of *Limulus* hemocyanin are characterized by different circular dichroism spectra. These are, however, not unambiguously associated with the aggregation-state changes in that the CD spectra were found to be sensitive to pH under conditions where the aggregation state was unaltered. The 24-subunit complex of *Limulus* hemocyanin was found to be similar in its functional properties to the native 48-subunit aggregate. No unique functional properties thus appear to be associated with the 48-subunit ensemble that is found only in horseshoe crabs. Upon dissociation to the level of dodecamers, the reverse Bohr effect, cooperatively, and modulation of oxygen affinity by NaCl are still present although diminished in magnitude. Taken together, these studies clearly indicate that the interactions that stabilize dodecamers are different in pH and ion sensitivity from the interactions that are involved in formation of the 24-subunit complex from dodecamers and that these in turn differ from the interactions that stabilize the 48-subunit complex. These results are consistent with other lines of evidence that indicate that interactions at these different levels are dominated by structurally and functionally distinct types of subunits.

The results reported here concern the dissociation and assembly of *Limulus polyphemus* hemocyanin and the functional consequences associated with changes in its aggregation state. Our study of the factors that govern the assembly and stabilization of this high molecular weight oxygen carrier has general significance in view of the many reactions of biological importance carried out by complex aggregates whose assembly may be similarly controlled by pH and specific-ion effects. We consider that hemocyanins are particularly good model systems for analysis of the role of specific effectors and specific types of subunits in both the assembly and the function of heteropolymers. Notably, functional consequences of partial dissociation of hemocyanins can be followed because in these proteins the dissociation products do not lose their capability to bind oxygen reversibly.

In the horseshoe crab *Limulus polyphemus* the native hemocyanin molecule is an aggregate of 48 subunits. Each of the subunits contains a single oxygen binding site composed of a pair of copper atoms whose ligation to the protein has been the subject of recent investigation (Solomon et al., 1982). Structural information on this protein was first obtained by Svedberg in his pioneering analytical ultracentrifugation studies. He showed that *Limulus* hemocyanin can exist in various discrete aggregation states, whose proportions are affected by both pH and ionic conditions (Svedberg & Hedenius, 1934; Svedberg & Heyroth, 1929). The sedimentation equilibrium studies of Johnson & Yphantis (1978) determined the native molecule to be a 48-subunit complex with a molecular weight of 3 160 000 and a sedimentation coefficient of 60 S.[1] Dissociation products with sedimentation coefficients of 37 and 24 S were determined to be 24-subunit and 12-subunit molecules with molecular weights of 1 690 000 and 856 000, respectively. The monomers have an average molecular weight of about 70 000. Structural and functional heterogeneity among the *Limulus* hemocyanin monomers has been extensively documented (Sullivan et al., 1974; Bonaventura et al., 1974; Lamy et al., 1979a; Brenowitz et al., 1981). Of particular interest in regard to the stepwise dissociation of *Limulus* hemocyanin is the fact that different types of subunits appear to play specific roles in the reassembly of

† From the Duke University Department of Biochemistry and Marine Biomedical Center, Duke University Marine Laboratory, Beaufort, North Carolina 28516. *Received June 21, 1983; revised manuscript received October 10, 1983.* Portions of this work are taken from the Ph.D. thesis of M.B. presented to Duke University. This work was supported by Grant PCM 79-06462 from the National Science Foundation. This paper is dedicated to our dear friend and colleague Professor Eraldo Antonini of the University of Rome, whose recent death was a personal and scientific loss.

* Address correspondence to this author at the Department of Biology, The Johns Hopkins University, Baltimore, MD 21218.

[1] Abbreviations: CDTA, (1,2-cyclohexylenedinitrilo)acetic acid; EDTA, ethylenediaminetetraacetate; EGTA, ethylene glycol bis(β-aminoethyl ether)-*N,N,N',N'*-tetraacetate; HIMDA, [*N*-(2-hydroxyethyl)imino]diacetic acid; *I*, ionic strength; k_{off}, oxygen dissociation rate constant; *n*, Hill coefficient; NTA, nitrilotriacetic acid; P_{50}, partial pressure of oxygen at 50% saturation; *s*, sedimentation coefficient in Svedbergs (S); Tris, tris(hydroxymethyl)aminomethane; CD, circular dichroism.

0006-2960/84/0423-0879$01.50/0

the aggregate (Bijlholt et al., 1979; Brenowitz et al., 1984). Our interest in further understanding the significance of subunit diversity in the structure and function of hemocyanins prompted us to reexamine the stepwise dissociation of *Limulus* hemocyanin and to examine systematically the reassembly process.

The oxygen-binding characteristics of *Limulus* hemocyanin are modulated by subunit interactions within the oligomer (Sullivan et al., 1974; Brouwer et al., 1977). As part of this study, we have established conditions under which the homotropic and heterotropic allosteric interactions of the native molecule can be compared to those of the 24- and 12-subunit dissociation intermediates. Circular dichroism spectroscopy was used to monitor the effect on tertiary structure brought about by changes in quaternary structure and by the dissociation of protons and Ca^{2+} from the protein under conditions where the aggregation state is constant. Our preliminary studies on the calcium dependence of the 48- to 24-subunit transition of *Limulus* hemocyanin were reported in an earlier paper (Brenowitz et al., 1980). The dissociation of *Limulus* hemocyanin was further investigated by a stopped-flow light-scattering technique that allows the time course of dissociation to be followed (Brouwer et al., 1981).

Considerable attention was focused on the calcium-dependent transition from 48- to 24-subunit oligomers, as the 48-subunit aggregate is unique to horseshoe crab hemocyanin. Two related Chelicerata, the scorpion *Androctonus* and the spider *Eurypelma*, have hemocyanins that immunochemically cross-react with *Limulus* hemocyanin and have similar subunit complexity yet only aggregate to 24-subunit oligomers (Lamy et al., 1979b,c). It was of interest to determine if the 48-subunit complex of *Limulus* hemocyanin has unique or physiologically adaptive functional or structural characteristics.

Materials and Methods

Protein Purification. Adult *Limulus*, collected around Beaufort, NC, or Woods Hole, MA, were bled by inserting a needle between the prosoma and opisthosoma and gently drawing the hemolymph into a syringe. The hemolymph was then centrifuged at 4 °C for 10 min at 17000 rpm to remove the fibrous clot. Native hemocyanin was purified by pelleting the hemocyanin from the hemolymph by preparative ultracentrifugation at 106000*g* for 2 h at 4 °C. The pellet was resuspended in $I = 0.1$ Tris-HCl containing 10 mM $CaCl_2$, pH 7.4. The purified hemocyanin was dialyzed at room temperature against 500 volumes of $I = 0.1$ buffer, prepared according to the recipes of Long (1961), for 24 h prior to the ultracentrifugation experiments. Tris was used between pH 7 and 9, cacodylic acid between pH 5.5 and 7, acetate from pH 5.5 to 4.5, formate from pH 4.5 to 4.0, and glycine below pH 4.0. Hemocyanin was stored at 4 °C prior to use.

Ultracentrifugation. Sedimentation velocity experiments were carried out in a Beckman Model E analytical ultracentrifuge. The sedimentation coefficients were calculated from the movement of the maximum ordinate of the schlieren boundaries and, for a few experiments conducted with a photoelectric scanner, from the midpoint of the absorbance tracings at 280 nm. Corrections of the sedimentation values to $s_{20,w}$ were by standard procedures with the assumption that $\bar{v} = 0.725$ as for other hemocyanins (Carpenter & Van Holde, 1973; Roxby et al., 1974). Protein concentrations were determined from the absorption at 280 and 340 nm with the extinction coefficient determined by Nickerson & Van Holde (1971).

Preparation of Dissociated and Reassembled Hemocyanin. The 24-subunit (37S) molecule was obtained by dialysis of native hemocyanin vs. pH 7.0, $I = 0.1$ Tris-HCl–10 mM EDTA. The 12-subunit (24S) molecule was obtained by dialysis vs. pH 5.0, $I = 0.1$ acetate–10 mM EDTA. Dissociation to monomers (5S) was accomplished by dialysis vs. pH 8.9, $I = 0.1$ Tris-HCl–10 mM EDTA.

Whole 48-subunit molecules (60S) were reassembled from 24-mers (37S) and dodecamers (24S) by dialysis vs. pH 7, $I = 0.02$ Tris-HCl–10 mM $CaCl_2$ buffer. To reassemble the 24-subunit molecules (37S) from unfractionated monomers (5S), samples were dialyzed vs. pH 7, $I = 0.02$ Tris-HCl–10 mM EDTA. To reassemble 12-subunit molecules (24S) from monomers, samples were dialyzed vs. pH 5, $I = 0.02$ acetate–10 mM EDTA. All dialysis was carried out at room temperature for at least 12 h.

A three-step procedure was used to reassemble 48-subunit (60S) molecules from monomers. First, monomers were dialyzed vs. the 37S reassembly buffer for 24 h. They were then transferred to $I = 0.02$ Tris-HCl, pH 7, buffer for 24 h. For the final step, the protein was transfered to $I = 0.02$, pH 7, 10 mM $CaCl_2$ buffer for 24 h. No increase in the amount of reassembled protein was observed when samples were dialyzed longer than 24 h in the final buffer. The percentage of each component obtained in the reassembly reactions was determined by projecting the schlieren patterns from the ultracentrifuge analysis onto graph paper and counting the number of squares under each peak. Correction for radial dilution was made in the usual manner.

Oxygen-Binding Measurements. Oxygen-equilibrium experiments were performed in tonometers by the method of Riggs & Wolbach (1956). Values of percent saturation were calculated on the basis of 340 nm absorbance changes.

Circular Dichroism. CD measurements were carried out on a Jobin Yvon Dichrograph Mark III spectrophotometer. Samples of hemocyanin prepared as described above were dialyzed vs. $I = 0.01$ buffers prior to scanning to reduce the background absorption of the buffer. Sedimentation velocity experiments showed that the sedimentation values of each of the aggregates were unchanged under these lower ionic strength conditions (data not shown). Path lengths of 0.1 cm and protein concentrations of 0.25 mg/mL were used. To eliminate error in the concentration determinations due to different amounts of scattering by the high molecular weight aggregates, concentrations were determined on samples that had been diluted with pH 9.0, $I = 0.2$ Tris-HCl–10 mM EDTA buffer, which induces dissociation into monomers. Molar ellipticity (per subunit) was calculated by using a mean residue weight (MRW) of 117.95, calculated on the basis of the amino acid composition reported by Ghiretti-Magaldi et al. (1966).

Measurement of the Rate of Hemocyanin Dissociation. The process of dissociation of hemocyanin oligomers can be followed by a stopped-flow light-scattering technique (Brouwer et al., 1981). The dissociation rates associated with specific transitions were determined by rapidly mixing hemocyanin solutions with buffers of varied composition. Hemocyanin solutions to be dissociated were dialyzed against $I = 0.01$ buffers (sample buffers), and dissociation was initiated by rapid mixing with an equal volume of $I = 0.2$ buffers (dissociation buffers) at either a different pH or containing a Ca^{2+} chelator. The pH after mixing the sample and dissociation buffers was within 0.1 unit of the initial pH of the dissociation buffer. The pH, the ionic strength, and the presence of either a chelator or Ca^{2+} in the dissociation buffer were selected to bring about the desired changes in aggregation state. The specific buffers used are described in the legends of Figures 6 and 7. The

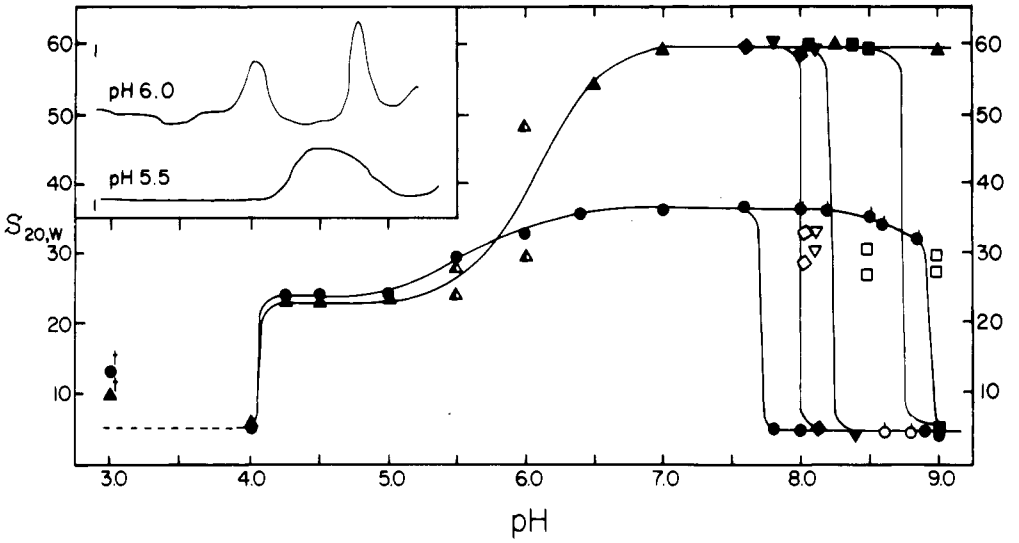

FIGURE 1: Dependence of *Limulus* hemocyanin aggregation on pH at ionic strength 0.1 to which the indicated ions were added. Buffers at each pH are as described under Materials and Methods: (▲) 10 mM $CaCl_2$; (■) 1 mM $CaCl_2$; (▼) 0.1 mM $CaCl_2$; (♦) 0.01 mM $CaCl_2$; (●) 10 mM EDTA; (tagged circles) 10 mM EDTA and 0.5 M NaCl. The open symbols represent components present in minor amounts. The schlieren patterns for the runs represented by the half-filled symbols at pH 5.5 and 6.0 are shown in the insert. Crosses (†) show solutions where A_{340} was lost. The protein concentration is 4.5 mg/mL for all experiments. (Insert) Schlieren profiles of the 60S to 24S dissociation in I = 0.1 cacodylic acid–10 mM $CaCl_2$. Sedimentation values are given in Figure 1 for each of the peaks. The pH 6.0 sample was run at 40 000 rpm while the pH 5.5 sample was run at 44 000 rpm. The meniscus is on the left.

changes in aggregation state were monitored as a decrease in the light-scattering intensity at 425 nm. The data are presented as first-order plots with the rates of reaction estimated according to

$$\ln \frac{V_t - V_\infty}{V_0 - V_\infty} = \ln \frac{\Delta V_t}{\Delta V_0} = -kt$$

where V_0, V_t, and V_∞ are relative digitized readings of photomultiplier output observed at the beginning, at time t, and at the end of the reaction, respectively. Analytical ultracentrifugation was used to establish the starting and end points of the transitions.

Determination of the Rate of Calcium Chelation. As a prerequisite for further analysis of Ca^{2+}-dependent hemocyanin dissociation, it was necessary to show that Ca^{2+} chelation was complete and not rate limiting. To verify experimentally complete Ca^{2+} chelation, a calcium indicator, murexide, was added to a concentration of A_{485} = 1.0 to pH 7 buffers containing either 10 mM $CaCl_2$ or 10 mM EDTA. Equal parts of the murexide buffers and identical buffers without indicator were mixed and scanned to obtain the Ca^{2+}-bound murexide spectrum (absorption maximum at 485 nm) and the Ca^{2+}-free murexide spectrum (maximum at 520 nm) under these conditions. The spectra of pH 7 buffer containing 25 mM EDTA, CDTA, NTA, or HIMDA mixed with pH 7, 10 mM $CaCl_2$–murexide solution were measured and compared with the control spectra above. These spectra were identical with the Ca^{2+}-free murexide control spectra, demonstrating complete calcium chelation. To determine the rate of Ca^{2+} chelation, the same experiments were performed in the stopped-flow spectrophotometer. The reaction was monitored by the decrease in A_{485} with the photomultiplier in the transmission mode. To determine the beginning and end points of the reaction, the Ca^{2+}-free and Ca^{2+}-bound murexide solutions described above were each introduced into the spectrophotometer, and the digitized voltage output of the photomultiplier was recorded for each solution. When the various chelator-containing buffers were mixed with the buffer containing 10 mM $CaCl_2$–murexide, the photomultiplier output at the end of each of the reactions was equal to that observed for the Ca^{2+}-free murexide solution. No Ca^{2+} dissociation curve could be obtained at even the fastest sweep rate (10 μs/sample point) of the analog to digital converter, showing that complete chelation of free Ca^{2+} occurs within the 2.3-ms dead time of the rapid-mixing apparatus.

Results

Ultracentrifuge Analysis of the Dissociation Reactions. Under the various buffer conditions studied, a total of four molecular weight components were observed, which will be referred to by their approximate sedimentation coefficients, 60 S, 37 S, 24 S, and 5 S. The molecular weight and number of constituent subunits of each component were described in the introduction. Figure 1 presents an overall picture of the pH and Ca^{2+} effects. The 60S to 5S transition occurs over a very narrow pH range and is dependent on the Ca^{2+} concentration (Figure 1). The predominant species present at alkaline pH in the presence of less than 10 mM Ca^{2+} are 60S and 5S molecules with partially resolved 37S and 24S peaks present in minor amounts at the transition pH values. The 60S molecule is also stabilized against dissociation at alkaline pH by increased ionic strength (Brouwer et al., 1981). In the following experiments, we attempt to differentiate between Ca^{2+}, pH, and ionic strength effects at varied stages of the dissociation process.

Native hemocyanin will dissociate into 37S molecules upon dialysis against pH 7, EDTA-containing buffer (Figure 1). Dialysis against buffers containing 100 mM $MgCl_2$ and 10 mM of the Ca^{2+}-specific chelator EGTA or containing 500 mM NaCl with 10 mM EDTA induced dissociation into 37S molecules. Magnesium ions and Na^+ are thus incapable of substituting for Ca^{2+} in stabilizing the 60S structure under these conditions.

The 37S to 5S dissociation also occurs over a very narrow range with a critical pH between 7.6 and 7.8 (Figure 1). No intermediate dissociation products were observed, although at pH 7.6 the 37S boundary is asymmetric toward the meniscus of the centrifuge cell (data not shown). With the addition of 0.5 M NaCl to the buffer the pH of the transition increased to between pH 8.8 and 9.0 (Figure 1) with the trailing edges

Table I: Reassembly of *Limulus* Hemocyanin[a]

initial conditions			final conditions		
reassembly	$s_{20,w}$ at $I = 0.1$	buffer	buffer	$s_{20,w}$ at $I = 0.02$	$s_{20,w}$ at $I = 0.1$
5S to 36S	5.25	pH 9 EDTA	pH 7 EDTA	35.9 (100)	35.6 (100)
24S to 36S	23.7	pH 5 EDTA	pH 7 EDTA	35.7 (100)	36.0 (100)
5S to 24S	5.25	pH 9 EDTA	pH 5 EDTA	32.9 (19) 22.6 (53) 8.0 (27)	17.2 (60) 5.2 (40)
5S to 24S	5.25	pH 9 EDTA	pH 5 $CaCl_2$	22.9 (20) 22.0 (52) 8.1 (27)	
36S to 60S	35.4	pH 7 EDTA	pH 7 $CaCl_2$	59.1 (81) 38.8 (19)	55.9 (8.0) 39.2 (92)
24S to 60S	24.7	pH 5 EDTA	pH 7 $CaCl_2$	58.6 (71) 39.0 (29)	54.0 (7.0) 37.1 (93)
24S to 60S	25.8	pH 5 $CaCl_2$	pH 7 $CaCl_2$	58.2 (72) 38.4 (28)	56.4 (7.0) 36.5 (93)
5S to 60S	5.25	pH 9 EDTA	pH 7 $CaCl_2$ 34 000 rpm	58.6 (39) 37.6 (61)	51.7 (6) 35.9 (94)
			24 000 rpm	57.5 (59) 38.0 (41)	52.6 (5.0) 35.1 (95)
			16 000 rpm	55.5 (54) 36.4 (46)	

[a] The last two columns refer to the $s_{20,w}$'s observed in $I = 0.02$ and 0.1 reassembly buffers, respectively. The percentage of each component is shown in parentheses following the sedimentation coefficient of the component. The EDTA and $CaCl_2$ concentrations are 10 mM. The initial protein concentration is 6 mg/mL.

of the boundaries showing increasing asymmetry at alkaline pH (data not shown).

Dissociation of native hemocyanin to 24S molecules occurs on dialysis upon lowering the pH to 5 with subsequent dissociation to 5S monomers occurring between pH 4.2 and 4.0 (Figure 1). Further lowering of the pH to 3 results in the denaturation of the protein, as evidenced by the loss of absorbance at 340 nm and a sharp increase in the sedimentation coefficient.

The 37S molecule, stable at pH 7 in EDTA-containing buffer, can also be dissociated into 24S intermediates by lowering the pH to 5. This interaction differs from the previously described dissociation reactions in that as the pH is lowered in the presence of EDTA, a symmetric boundary of decreasing sedimentation coefficient is observed (Figure 1), with no indication of boundaries corresponding to monomers (data not shown). This reaction is completely reversible (see Table I). These observations suggest the presence of a pH-dependent, rapid equilibrium. To test this, the protein-concentration dependence of the equilibrium was checked at pH 7.0, 6.0, and 5.0. The weight-average sedimentation coefficient as a function of protein concentration calculated from the monomer–dimer equations derived by Gilbert & Gilbert (1973) was fit to the data by using a nonlinear least-squares program and by assuming 37S and 22S (the estimated s^0 value of the 24S component) as the sedimentation values for the dimer and monomer, respectively (Figure 2). The results show that the transition is clearly a rapid monomer–dimer equilibrium with the hemocyanin predominantly in the 37S and 24S forms at pH 7 and 5, respectively.

The dissociation of the 60S molecule (in 10 mM $CaCl_2$) to 24S molecules occurs without calcium chelation over the same pH range as the above-described 37S to 24S dissociation (Figure 1). In this case, however, both 60S and 37S boundaries are observed at an intermediate stage of the dissociation;

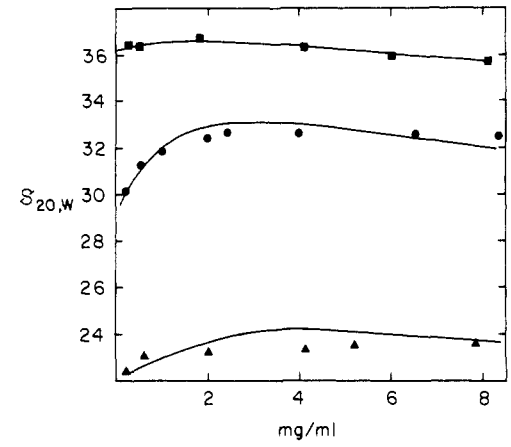

FIGURE 2: Dependence of $s_{20,w}$ on protein concentration for the 37S–24S interaction in $I = 0.1$ buffers (see Materials and Methods) containing 10 mM EDTA: (■) pH 7; (●) pH 6; (▲) pH 5. The solid lines are the curves calculated from the monomer–dimer equilibrium theory (see text). The best fit values of the equilibrium constant, K, and the nonideality constant, g, which were generated by the least-squares analysis are 2744 L/g ± 526 and 0.0040 L/g ± 0.0001 at pH 7, 8.11 ± 1.07 and 0.0113 ± 0.0014 at pH 6, and 0.116 ± 0.059 and 0.166 ± 0.0077 at pH 5.

and a broad asymmetrical peak whose velocity is intermediate to the 37S and 24S molecules appears as the pH is further lowered (Figure 1, insert). At pH 5, a symmetrical peak that is identical with that observed at pH 5 in 10 mM EDTA is observed. From these results, it appears that the dissociation of 60S to 24S molecules in the presence of $CaCl_2$ follows a pathway of dissociation to 37S molecules, which in turn dissociate to 24S dodecamers.

Ultracentrifuge Analysis of Reassembly Reactions. When unfractionated monomers at pH 9 are dialyzed vs. pH 7, 10 mM EDTA-containing buffer, 37S molecules are observed at

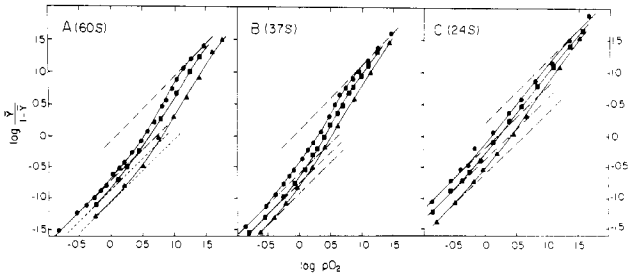

FIGURE 3: (A) Hill plots of oxygen binding of 60S molecules with varied concentrations of NaCl in pH 7, I = 0.1 Tris–10 mM $CaCl_2$: (●) no added NaCl; (■) 0.5 M NaCl; (▲) 2 M NaCl. (B) 37S molecules in pH 7, I = 0.1 Tris–10 mM EDTA: (●) no added NaCl; (■) 0.5 M NaCl; (▲) 1.5 M NaCl. (C) 24S molecules in pH 5, I = 0.1 acetate–10 mM EDTA: (●) no added NaCl; (■) 0.5 M NaCl; (▲) 1.5 M NaCl. The P_{O_2} is expressed in millimeters of Hg. Protein concentration is 4.5 mg/mL.

both low and moderate ionic strength (Table I). These 37S molecules will be referred to as "reassembled 37S molecules" to distinguish them from the "native 37S molecules" produced by dissociation of native hemocyanin. In contrast, when monomers are dialyzed vs. pH 5 buffer, only partial assembly to 24S dodecamers occurs (Table I). The 17.2S peak observed at I = 0.1 has a sedimentation coefficient that approximately corresponds to a hexamer of 5S monomers.

The reassembly of 60S from 37S and 24S molecules is Ca^{2+} dependent. The presence or absence of $CaCl_2$ in the initial buffer at pH 5 does not influence formation of 60S molecules (Table I). The reassembly to 60S molecules is hindered at I = 0.1 or above and occurs with a high yield only at or below I = 0.02 (Table I). Even at I = 0.02, there is appreciable hysteresis. To test if the inhibition at I = 0.1 is specific to the Tris reassembly buffer, a 37S sample was dialyzed against ionic strength 0.02 Tris buffer to which was added (a) 10 mM $CaCl_2$, (b) 10 mM $CaCl_2$ and 80 mM NaCl, or (c) 90 mM $CaCl_2$. Only under condition a does reassembly to 60S molecules occur. Conditions b and c yield 5 and 8% reassembly, respectively, similar to the results obtained upon dialysis against I = 0.1 Tris–10 mM $CaCl_2$ (Table I). These results show that the inhibition of reassembly appears to be a general ionic strength effect.

The reassembly of 60S molecules from reassembled 37S molecules shows the same dependence on ionic strength as the native 37S molecules to 60S assembly (Table I). However, in the first case, the proportion of 60S material shows a strong dependence on rotor speed with an elevated base line between the 60S and 37S peaks (Table I; Brenowitz, 1982). Since only the reassembled 37S molecules show this behavior (which is characteristic of a pressure-dependent equilibrium with the 60S form), these reassembly products are clearly not identical with the native 37S molecules.

Oxygen-Binding Properties. Identical sedimentation coefficients for oxygenated and deoxygenated molecules were found under all the conditions described in Figure 3, indicating that the aggregation state of the hemocyanin did not change during the oxygen-binding experiments. The calcium-dependent dissociation of 60S to 37S molecules causes a small increase in oxygen affinity but no loss of cooperativity (Figures 3 and 4). The 37S molecule shows a pronounced reverse Bohr effect, although of somewhat reduced magnitude compared to that of the 60S molecule (Figure 4). The oxygen-binding affinities of native and reassembled 37S hemocyanin molecules are very similar, although the reassembled hemocyanin shows slightly less cooperativity (n = 1.9 and 1.6, respectively).

Dissociation from the 37S to the 24S state alters both the affinity and the cooperativity of the protein (Figures 3 and

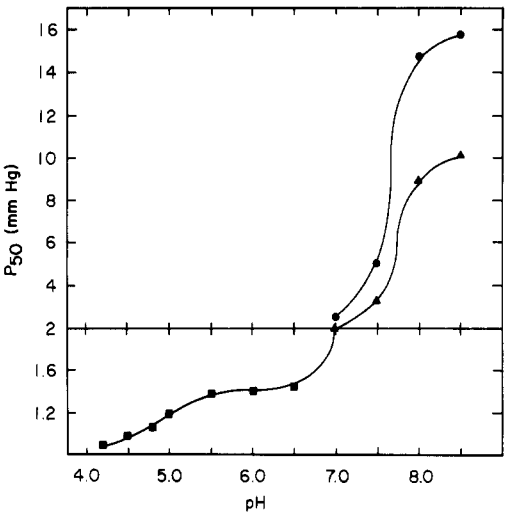

FIGURE 4: pH dependence of oxygen affinity of the 60S molecule in I = 0.1 buffers (see Materials and Methods), 10 mM $CaCl_2$ and 0.5 M NaCl (●), 37S molecules in I = 0.1 buffers, 10 mM EDTA and 0.5 M NaCl (▲), and the 37S to 24S transition (pH 7 to 5) and for the 24S molecule (pH 5 to 4.2), in I = 0.1 buffers (10 mM EDTA) (■). Protein concentration is 4.5 mg/mL.

4). Figure 4 shows that a reverse Bohr effect of reduced magnitude compared to that of the native molecule is observed during the transition from pH 7 to 5. A reverse Bohr effect is also observed between pH 5 and 4.2, conditions under which the dodecamer is stable. Calcium ions have little effect on the oxygen-binding properties of the 24S molecule (data not shown). As previously shown (Brouwer et al., 1977), chloride ions specifically diminish the oxygen affinity of intact (60S) molecules. Figure 3 illustrates this effect and demonstrates that increasing concentrations of NaCl have a similar effect on the 37S and 24S molecules.

Circular Dichroism. Far-UV CD spectroscopy was used to detect changes in tertiary structure that accompany changes in quaternary structure of *Limulus* hemocyanin. Approximately equal increases in ellipticity accompany the Ca^{2+}-dependent 60S to 37S and 60S to 5S dissociations (Figure 5A,B). Similarly, the pH-dependent changes in the CD spectra are also equivalent when no dissociation is involved (60S molecules in $CaCl_2$-containing buffer) and when 37S molecules dissociate to 5S monomers (compare the two upper spectra and two lower spectra of Figure 5A,B). Thus, changes in ellipticity are not dependent on the specific changes in aggregation state induced by either protons or Ca^{2+}. The spectra of the 37S and 24S molecules at pH 7 and 5, respectively, are practically indistinguishable (Figure 5A,C). Chelation of Ca^{2+} has virtually no effect on the spectra of the dodecamer at pH 5 (Figure 5C). In no case were there shifts in the peak positions.

Kinetics of Hemocyanin Dissociation. Stopped-flow light-scattering experiments were performed to gain further insight into the factors that stabilize various aggregation states of *Limulus* hemocyanin. Under the experimental conditions employed in this study, the measured intensity of the scattered light is a linear function of the hemocyanin's molecular weight (data not shown). The linearity of the scattering intensity with protein concentration was previously demonstrated by Brouwer et al. (1981). That the rate of free-calcium chelation is instantaneous relative to the rate of protein dissociation is shown under Materials and Methods.

When 60S hemocyanin is mixed with pH 9 buffer containing 25 mM EDTA, complete dissociation to monomers occurs with the apparent rate of the process increasing with time (Figure 6A). Increasing the ionic strength with added

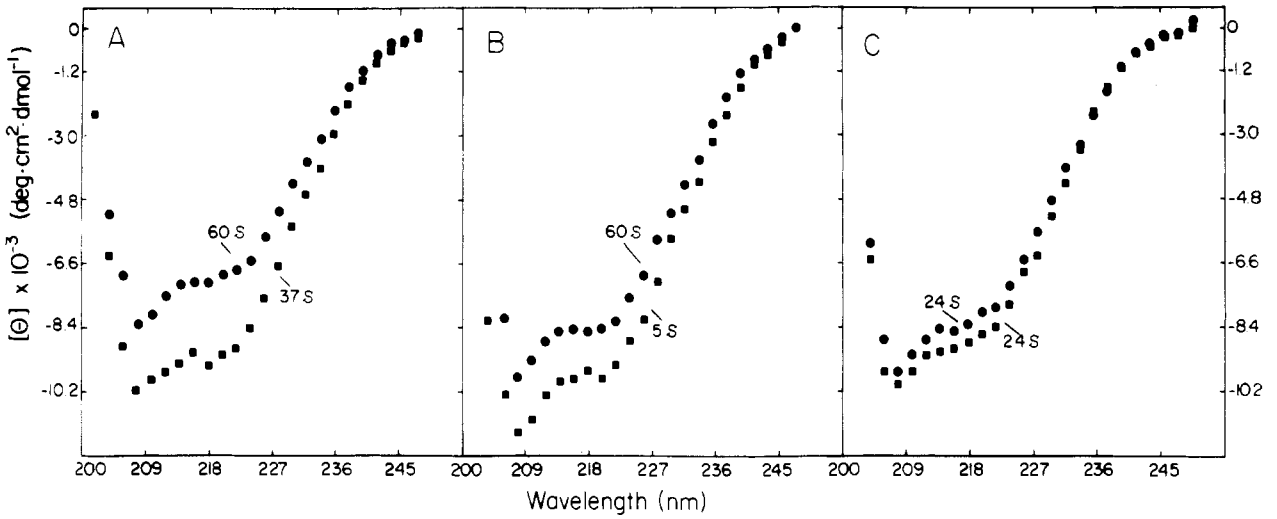

FIGURE 5: Far-UV CD spectra of *Limulus* hemocyanin. (A) (●) 60S molecules in I = 0.01 Tris-HCl, pH 7.0–10 mM $CaCl_2$; (■) 37S molecules in I = 0.01, pH 7.0–1 mM EDTA. (B) (●) 60S molecules in I = 0.01 Tris-HCl, pH 9.0–10 mM $CaCl_2$; (■) 5S monomers in I = 0.01, pH 9.0–1 mM EDTA. (C) (●) 24S molecules in I = 0.01 acetate, pH 5.0–10 mM $CaCl_2$; (■) 24S molecules in I = 0.01, pH 5.0–1 mM EDTA.

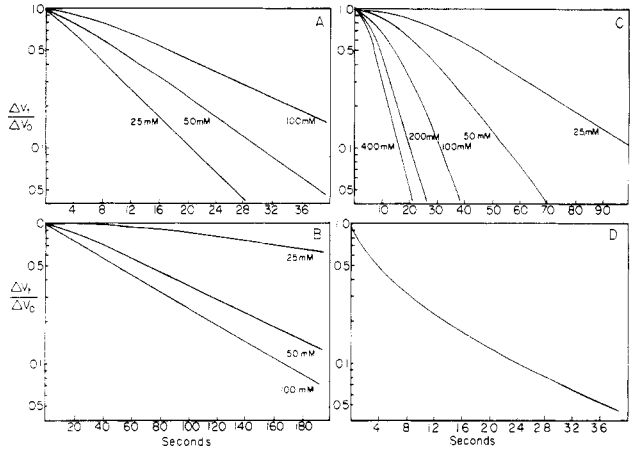

FIGURE 6: (A) First-order plots of the 60S to 5S dissociation. In these experiments, equal volumes of sample and dissociation buffers were mixed, and the decrease in A_{425} was monitored. The protein concentration after mixing is 2.2 mg/mL. The 60S molecules are in pH 7.0, I = 0.01 Tris-HCl–10 mM $CaCl_2$. Dissociation buffer is pH 9.0, I = 0.2 barbitol, with 25, 50, or 100 mM EDTA as indicated. (B) The same as (A), except the dissociation buffer was made 0.2 M NaCl. (C) First-order plot of the 60S to 37S dissociation as a function of EDTA concentration. The 60S molecule in pH 7, I = 0.01 Tris-HCl–10 mM $CaCl_2$ is dissociated by mixing with pH 7.0, I = 0.2 Tris-HCl with the indicated EDTA concentration. The protein concentration after mixing is also 2.2 mg/mL for panels B–D. (D) First-order plot of the 37S to 5S dissociation. The 37S molecule in pH 7.0, I = 0.01 Tris-HCl–10 mM EDTA was rapidly mixed with dissociation buffer of pH 9.0, I = 0.2 barbitol–25 mM EDTA.

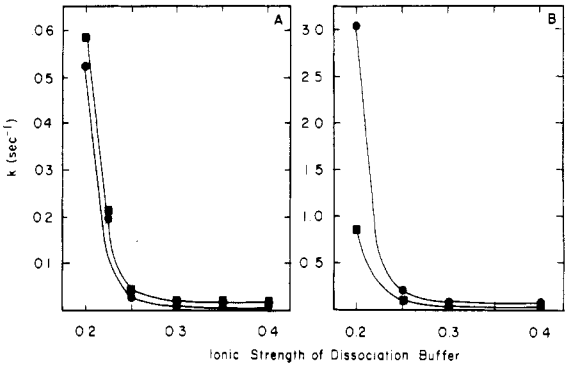

FIGURE 7: Effect of increasing ionic strength on the first-order rate constant of the (A) 60S to 5S and (B) 37S to 5S dissociations. The 60S hemocyanin in pH 7.0, I = 0.01 Tris-HCl–10 mM $CaCl_2$ or the 37S hemocyanin in pH 7.0, I = 0.01 Tris-HCl–10 mM EDTA is rapidly mixed vs. a dissociation buffer of pH 9.0, I = 0.2 barbitol–50 mM EDTA brought to the desired ionic strength with NaCl. (●) Initial 10% of the reaction; (■) final 10%.

NaCl decreases both the initial and final phases of the reaction equivalently, with the greatest decrease in apparent rate occurring between I = 0.2 and 0.25 (Figure 7A). Sodium chloride and sodium acetate were equally effective in decreasing the dissociation rate, ruling out a specific chloride effect.

The rate of dissociation of 60S molecules to 5S monomers decreases with increasing EDTA concentration in I = 0.2 dissociation buffer; while in I = 0.4 dissociation buffer, increasing the EDTA concentration brings about an increase in the dissociation rate (Figure 6A,B). This suggests that in I = 0.2 buffer the EDTA makes a substantial contribution to the total ionic strength of the solution. At I = 0.4, the transition is minimally sensitive to changes in ionic strength (Figure 7A), and under these conditions an EDTA-induced facilitation of dissociation is observed.

Several experiments were performed to resolve the characteristics of Ca^{2+}-dependent and Ca^{2+}-independent dissociation reactions. As previously established, the 60S to 37S transition can be brought about at pH 7 by removal of Ca^{2+}. The apparent rate of the dissociation process was found to increase as the reaction proceeds (Figure 6C). The dissociation at this pH is 1 order of magnitude slower, at equal EDTA concentrations, than the 60S to 5S transition (compare panels A and C of Figure 6) and shows a greatly reduced sensitivity to ionic strength (data not shown). The apparent rate of the initial phase of the reaction (defined as the first 10%) increases linearly with increasing EDTA concentration (Figure 8), reminiscent of the effect of EDTA on the 60S to 5S dissociation at I = 0.4 (Figure 6B).

To show that it is the Ca^{2+}-free chelator rather than the complexed chelator that facilitates dissociation, experiments were performed with varied concentrations of EDTA to which $MgCl_2$ was added to maintain a constant concentration of uncomplexed chelator. Dissociation buffers with chelator to $MgCl_2$ ratios (mM/mM) of 50/25, 100/75, 200/175, and 300/275 were used to maintain an initial uncomplexed chelator concentration of 25 mM. As shown in Figure 8, the apparent rate of dissociation following mixture of the 60S material with these buffers was the same as that seen when the dissociation buffer contained only 25 mM EDTA, despite the increase in

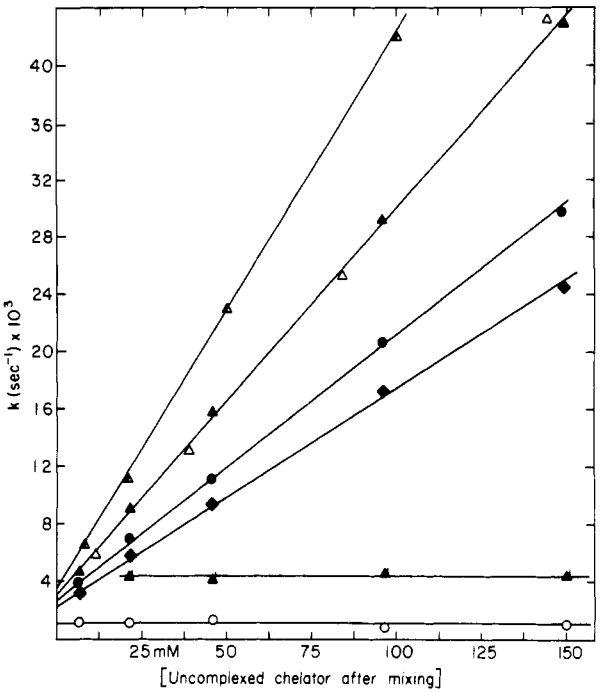

FIGURE 8: Effect of calcium affinity and concentration of chelator on 60S to 37S dissociation. Experimental conditions are as in Figure 6C. The values of k (s^{-1}) are the pseudo-first-order rate constants for the initial 10% of the reaction. The uncomplexed chelator concentration is that portion of the chelator in solution that is not complexed with calcium ions after mixing of the sample and dissociation buffers in the stopped-flow apparatus. This assumes complete chelation of the free calcium present in the sample buffer. For example, when 10 mM $CaCl_2$ in the sample buffer is mixed with an equal volume of dissociation buffer containing 25 mM EDTA, the uncomplexed chelator concentration is 7.5 mM. (▲) EDTA in the dissociation buffer and 10 mM $CaCl_2$ in the sample buffer (as in Figure 7C); (△) 25 mM $CaCl_2$ in the sample buffer; (half-filled triangles) 1 mM $CaCl_2$ in the sample buffer. (Tagged triangles) EDTA to $MgCl_2$ ratios as described in the text. In this case, the Mg–EDTA complexing was not considered when calculating the uncomplexed chelator concentration. In the following experiments, different calcium chelators were employed in the dissociation buffer: (●) NTA; (♦) HIMDA; (○) CDTA. The calcium affinity constants for the chelators are log K = 13.6 (CDTA), 10.6 (EDTA), 6.5 (NTA), and 4.7 (HIMDA) (Perrin & Dempsey, 1974; Martell & Smith, 1977). The second-order dissociation constants calculated from the slopes of the lines are 1.81 s^{-1} mol^{-1} (EDTA), 1.07 s^{-1} mol^{-1} (NTA), and 1.03 s^{-1} mol^{-1} (HIMDA).

the total chelator concentration.

When a series of chelators of decreasing Ca^{2+} affinity was studied, the increase in the initial dissociation rate was found to be linear with increasing chelator concentration in each case (Figure 8). Changing the protein concentration over a 5-fold range in concentration had no effect on the apparent rate of dissociation (data not shown), confirming that these processes can be analyzed by pseudo-first-order kinetics (the chelator in all cases studied is in far excess of the hemocyanin but not in far excess of calcium). As the Ca^{2+} affinity of the chelator decreased, the apparent rate of the 60S to 37S dissociation also decreased (Figure 8). Extrapolation to zero chelator concentration yields a non-zero intercept of approximately 2.7 $\times 10^{-3}$ s^{-1} (Figure 8). This value is an approximation of the intrinsic rate of the 60S to 37S dissociation without facilitation of Ca^{2+} dissociation by the chelators, i.e., the limiting condition where Ca^{2+} is freely diffusing from the protein into a "zero Ca^{2+}" solution. A second-order rate constant for the reaction in which the chelator interacts with protein can be calculated from the relationship, $k' = k/[\text{chelator}]$, where k is the pseudo-first-order rate constant. The values of k' (obtained for each chelator from the slopes of the lines of Figure 8) vary directly with the Ca^{2+} affinities of the chelators studied (Figure 8, legend).

If the observed facilitation of dissociation by the chelators were due to the formation of a chelator–Ca^{2+}–protein transition complex, it would be expected that a sterically hindered chelator might not be able to form a transient complex with the Ca^{2+} bound to the hemocyanin and, hence, would not facilitate dissociation. The compound CDTA has a high Ca^{2+} affinity, binding Ca^{2+} with tetraacetate ligands as does EDTA. The significant difference between EDTA and CDTA is the greater bulk and rigidity of the cyclohexane backbone of CDTA. Upon a rapid mixing with this chelator, the 60S to 37S dissociation was found to be independent of chelator concentration. The dissociation rate was, moreover, similar to the "intrinsic dissociation rate" extrapolated from the other chelators (Figure 8). This chelator, as hypothesized, appears unable to form the postulated protein–Ca^{2+}–chelator ternary complex that facilitates protein dissociation.

The 60S to 37S dissociation at pH 7 is autocatalytic with either 1, 10, or 25 mM $CaCl_2$ in the sample buffer (data not shown). The dependence on chelator concentration is equivalent whether 10 or 25 mM $CaCl_2$ is present in the sample buffer (Figure 8). However, the overall rate of the process is faster when the concentration of $CaCl_2$ in the sample buffer is reduced to 1 mM (Figure 8). This implies that some low-affinity sites that are not saturated at 1 mM $CaCl_2$ affect the stability of the 60S molecule.

Calcium-induced stabilization is not a factor in the 37S to 5S dissociation that is brought about by a pH jump from 7 to 9 in EDTA-containing buffer. This dissociation is 2 orders of magnitude faster than the 60S to 37S transition at comparable EDTA concentrations (Figure 6C,D). The apparent rate of the 37S to 5S dissociation process decreases over the course of the reaction. The process is 1 order of magnitude faster than the 60S to 5S transition (brought about by calcium chelation *and* a pH jump) although the dissociation rate has a similar dependence on ionic strength (Figure 7).

Discussion

From the results presented in this paper we can conclude that there is a hierarchy of structural interactions within the 48-subunit molecule of native *Limulus* hemocyanin. The dissociation from whole molecules to half-molecules has a minimal effect on the oxygen-binding properties of *Limulus* hemocyanin. Upon dissociation to the level of dodecamers, the reverse Bohr effect, cooperativity, and modulation of oxygen affinity by NaCl are diminished in magnitude but are still observed, showing that the subunit interactions responsible for the allosteric control of oxygen binding of *Limulus* hemocyanin are still present at this level of dissociation. The specificity of calcium ions in the stabilization of the native 48-subunit complex contrasts with the nonspecific stabilization by monovalent ions of the 24-subunit complex. This can in turn be differentiated from the functional effect of chloride ions on the oxygen affinity of the protein. It is clear that in this heteropolymer there are interactions between subunits with varied pH and specific-ion sensitivities that are responsible for linking the monomers within dodecamers, formation of 24-subunit complex from dodecamers, and formation of the native 48-subunit complex from the 24-subunit ensemble. On the basis of immuno electron microscopy studies, Lamy et al. (1984) have proposed a model of the quaternary structure of *Limulus* hemocyanin in which specific subunits are at the interfaces between different levels of aggregation. We would expect that the characteristics of the various dissociation and reassembly reactions studied in this paper would be reflected

by the self-assembly properties of those subunits localized at the interface of the dissociating aggregates. Results of experiments designed to test this hypothesis will be presented in a future publication (Brenowitz et al., 1984).

Calcium ions are clearly required to stabilize the interactions between 24-subunit (37S) aggregates, which allow for formation of the 48-subunit (60S) native molecule. The 24-subunit molecules are remarkably similar in their functional properties to the 48-subunit molecules. The absence of a calcium ion requirement for cooperative oxygen binding has been extensively documented for a number of arthropod hemocyanins and is clearly the case for *Limulus* hemocyanin [for examples, see Klarman & Daniel (1977) and Van Holde & Brenowitz (1981)]. However, recent studies by M. Brouwer (personal communication) indicate that calcium at concentrations higher than those studied here does act as an allosteric modulator and alters the degree of cooperativity in oxygen binding by 60S *Limulus* hemocyanin.

One possible mechanism for calcium ion stabilized aggregation, which has been suggested for erythrocruorins, is that Ca^{2+} is able to cross-link negative groups of potentially interacting dissociation products (Antonini & Chiancone, 1977). The inability of Mg^{2+} to substitute for Ca^{2+} in stabilization of 60S *Limulus* hemocyanin may be due to the smaller ion being unable to form the cross-linking bridge. Direct studies of calcium binding (Kuiper et al., 1979; Anderson et al., 1982; unpublished results from this laboratory) indicate that arthropod hemocyanins typically possess a small number of high-affinity calcium binding sites per subunit ($K = 10^4$–10^5 M^{-1}) and a large number of low-affinity sites ($K = 10^2$–10^3 M^{-1}). The stability of the 48-subunit molecule in 10 μM calcium (Figure 1) indicates that the high-affinity sites are responsible for the stabilization of the 48-subunit aggregate of *Limulus* hemocyanin. These would be saturated at the physiological concentration of calcium in the hemolymph ($\sim$10 mM; Robertson, 1970).

The cooperative oxygen binding by the 12-subunit dissociation product indicates that the intersubunit contacts necessary for homotropic interactions are still present in isolated dodecamers. The cooperativity of the dodecamer was not unexpected in that Brouwer et al. (1977) have shown that the hexamer can be considered as the allosteric unit under most conditions. In these studies, the depression of the oxygen affinity of the 48-mer by chloride ions was described by a concerted two-state model, with the assumption that chloride both changes the allosteric equilibrium constant between the low- and high-affinity states and also lowers the affinity of the low-affinity "T state" for oxygen (Brouwer et al., 1977). We observe a NaCl-dependent depression of the affinity of the T states of the 24- and 12-subunit aggregates as well (Figure 3). It is clear that the "chloride effect" characteristic of the native 48-subunit molecule is also exhibited by the 24-subunit and dodecameric molecules.

The dissociations of 48-, 24-, and 12-subunit aggregates to monomers are highly cooperative processes, which are independent of protein concentration over the ranges examined. There is an appreciable amount of hysteresis in the reassembly reactions, indicating that these interactions should not be regarded as simple equilibria. The concept of "microheterogeneity", introduced to account for similar behavior in molluscan hemocyanins and high molecular weight hemoglobins, explains dissociation patterns by predicting that at each aggregation state discrete populations of molecules are present, each of which undergoes cooperative dissociation at slightly different pH values (Konings et al., 1969; Engelborghs & Lontie, 1973; Siezen & Van Driel, 1973; Antonini & Chiancone, 1977). This explanation appears applicable to *Limulus* hemocyanin, whose subunits differ greatly in pH and specific-ion sensitivity. While it is not certain if heterogeneity exists at the 48-, 24-, or 12-subunit level of aggregation, such heterogeneity could explain the dissociation patterns. In only one transition for *Limulus* hemocyanin, the dissociation of the 24-mer to the dodecamer, does the reaction appear to be a true equilibrium. Hence, the interactions between the dodecamers may be constant in a hypothetical population of otherwise heterogeneous molecules.

The reassembly of *Limulus* hemocyanin is a complex process. The lack of residual monomers and "dead-end" intermediates in reassembly to 24-mers argues for a high degree of subunit specificity in the reassembly process. If incorrect intermediates are formed during reassembly, then subunit exchange as demonstrated by Bijlholt et al. (1979) must occur until the final, stable aggregate is formed. Although reassembly of the heterogeneous unfractionated monomers into 24-mers can be accomplished efficiently, it is not clear if a single type of 24-mer is formed or if reassembly results in a number of types of 24-mers, each having slightly different subunit composition. The dependence on pressure of the proportion of 48-mers formed from reassembled 24-mers and the lack of such dependence on the proportion of 48-mers formed from native 24-mers suggest that the two forms are, at least, slightly different. This could be due to irreversible conformational changes in the subunits upon dissociation.

Comparison of the dissociation and reassembly properties of the 24-subunit intermediate of *Limulus* hemocyanin with those of the 24-subunit native hemocyanin of *Eurypelma* shows similarities in the effect of pH, the effect of monovalent and divalent cations, and an absence of concentration dependence (Decker et al., 1980). The 12-subunit intermediates of *Eurypelma* and *Limulus* are not stable at alkaline pH. A significant difference is that the rates of dissociation and reassembly of *Eurypelma* hemocyanin (on the order of days) are much slower than those observed for *Limulus* under similar conditons (a few minutes). It is possible that, at the 24-subunit level, the two proteins have a common mechanism of dissociation and reassembly even though the processes proceed at substantially different rates. The large difference in dissociation rates may explain why a greater number of stable dissociation intermediates have been identified with *Eurypelma* hemocyanin (Markl et al., 1981).

It is clear that there are changes in the tertiary structure of the *Limulus* hemocyanin subunits associated with proton and calcium ion binding. These changes are not dependent on specific aggregation-state changes. The far-UV CD spectra of *Limulus* hemocyanin are also very similar in shape to those reported for the dodecamers and hexamers isolated from *Callinectes* and *Cherax* hemocyanins (Hamlin & Fish, 1977; Herskovits et al., 1981; Marlborough, 1979). No conformational changes were reported to occur on dissociation of these hemocyanins to monomers. The changes observed in the intensity of the spectra when conditions are altered for *Limulus* hemocyanin may be involved with the higher aggregation state of this protein.

The kinetics of the 48-subunit to 24-subunit and 24-subunit to monomer dissociation reactions differ in their rate, time course, and dependence on ionic strength. The kinetics of the 48-subunit to monomer dissociation appear to be limited by the Ca^{2+}-dependent 48-mer to 24-mer dissociation. However, the dependence of the 48-subunit to monomer transition on ionic strength is very similar to that found for the 24-mer to

monomer transition. These results suggest that the complete dissociation of the 48-subunit structure proceeds in a stepwise fashion, with the rate-limiting Ca^{2+}-dependent dissociation to 24-mers followed by a faster dissociation of 24-mers to monomers. Although 48-subunit molecules are stable in 1 mM $CaCl_2$, the difference between dissociation rates for samples in 1 and 10 mM $CaCl_2$ indicate that low-affinity calcium binding sites are important in additional stabilization of the 48-mer. The autocatalytic time course during the dissociation of the 48-subunit complex to the 24-subunit level is indicative of cooperative interactions between the various calcium binding sites. The dependence of the apparent rate of the dissociation process on the concentrations of various chelators shows that the rate-limiting step in the dissociation of the 48-subunit complex to the 24-subunit level involves calcium ion dissociation rather than an associated conformational change of the protein. If the latter were rate limiting, then the dissociation would be independent of chelator concentration and affinity.

From a physiological point of view, it is not clear what benefit horseshoe crabs derive from a 48-subunit oligomer compared to the immunochemical related 24-subunit hemocyanins of the scorpion, *Androctonus*, and the spider, *Eurypelma* (van Bruggen et al., 1980). As the oxygen-binding properties of the 48-mer and 24-mer of *Limulus* hemocyanin are not very different, could the fluctuations in temperature, salinity, and oxygen availability that are encountered by *Limulus* during the part of its life cycle it spends in the estuary affect the structure of the molecule? The blood pH of the hemolymph ranges from 7.1 to 7.55 (Johansen & Petersen, 1975). This pH range is well within the range of the pH stability of both the 48-mers and 24-mers, even at the physiologically low (0.1) ionic-strength conditions used in the stability determinations. Snyder & Mangum (1982) have shown that the viscosity and colloid osmotic pressure of solutions of *Limulus* 48-mers are much lower than those of solutions of dissociated subunits. These data suggest a physiological reason for large hemocyanin aggregates but do not distinguish between the effect of 48-subunit rather than 24-subunit aggregates on these parameters. This apparent lack of a clear advantage to the horseshoe crab of a 48-subunit over a 24-subunit molecule suggests that the 48-subunit structure is perhaps an evolutionary relic that has lost its functional significance over time. This view is supported by the fact that among the arthropods it is only the very primitive Xiphosurans that contain these large molecules and more "advanced" spiders have smaller aggregates (Markl & Kempter, 1981). Thus, the environmental stress that hypothetically necessitated the 48-subunit complex may no longer be encountered by *Limulus* in its contemporary habitat.

Acknowledgments

Some of the ultracentrifuge experiments were performed at the Marine Biological Laboratory, Woods Hole, MA, with the assistance of K. E. Van Holde. We are grateful to Jacqueline Reynolds for her help in performing the circular dichroism studies and to Marius Brouwer for a critical review of the manuscript.

Registry No. Ca, 7440-70-2; NaCl, 7647-14-5; O_2, 7782-44-7; EDTA, 60-00-4; CDTA, 13291-61-7; NTA, 139-13-9; HIMDA, 93-62-9.

References

Anderson, T., Chiancone, E., & Forsen, S. (1982) *Eur. J. Biochem. 125*, 103–108.

Antonini, E., & Chiancone, E. (1977) *Annu. Rev. Biophys. Bioeng. 6*, 239–271.

Bijlholt, M., van Bruggen, E. F. J., & Bonaventura, J. (1979) *Eur. J. Biochem. 95*, 399–405.

Bonaventura, C., Sullivan, B., Bonaventura, J., & Bourne, S. (1974) *Biochemistry 13*, 4784–4789.

Brenowitz, M. (1982) Ph.D. Thesis, Duke University, Durham, NC.

Brenowitz, M., Van Holde, K. E., Bonaventura, C., & Bonaventura, J. (1980) *Fed. Proc., Fed. Am. Soc. Exp. Biol. 39*, 1768.

Brenowitz, M., Bonaventura, C., Bonaventura, J., & Gianazza, E. (1981) *Arch. Biochem. Biophys. 210*, 748–761.

Brenowitz, M., Bonaventura, C., & Bonaventura, J. (1984) *Arch. Biochem. Biophys.* (in press).

Brouwer, M., Bonaventura, C., & Bonaventura, J. (1977) *Biochemistry 16*, 3897–3902.

Brouwer, M., Bonaventura, C., & Bonaventura, J. (1981) *Biochemistry 20*, 1842–1848.

Carpenter, D. E., & Van Holde, K. E. (1973) *Biochemistry 12*, 2231–2238.

Decker, H., Schmid, R., Markl, J., & Linzen, B. (1980) *Hoppe-Seyler's Z. Physiol. Chem. 361*, 1707–1717.

Engelborghs, Y., & Lontie, R. (1973) *J. Mol. Biol. 77*, 577–587.

Ghiretti-Magaldi, A., Nuzzolo, C., & Ghiretti, F. (1966) *Biochemistry 5*, 1943–1951.

Gilbert, L. M., & Gilbert, G. A. (1973) *Methods Enzymol. 27D*, 273–306.

Hamlin, L. M., & Fish, W. (1977) *Biochim. Biophys. Acta 491*, 46–52.

Herskovits, T. T., Erhunmwunsee, L. J., San George, R. C., & Herp, A. (1981) *Biochim. Biophys. Acta 667*, 44–58.

Johansen, K., & Petersen, J. A. (1975) in *Eco-Physiology of Estuarine Organisms* (Vernberg, F. J., Ed.) pp 129–145, University of South Carolina Press, Columbia, SC.

Johnson, M., & Yphantis, D. (1978) *Biochemistry 17*, 1448–1455.

Klarman, A., & Daniel, E. (1977) *J. Mol. Biol. 115*, 257–261.

Konings, W. N., Siezen, R. J., & Gruber, M. (1969) *Biochim. Biophys. Acta 194*, 376–385.

Kuiper, H. A., Forlani, L., Chiancone, E., Antonini, E., Brunori, M., & Wyman, J. (1979) *Biochemistry 18*, 5849–5854.

Lamy, J., Lamy, J., Weill, J., Bonaventura, J., Bonaventura, C., & Brenowitz, M. (1979a) *Arch. Biochem. Biophys. 196*, 324–339.

Lamy, J., Lamy, J., Weill, J., Markl, J., Schneider, H.-J., & Linzen, B. (1979b) *Hoppe-Seyler's Z. Physiol. Chem. 360*, 889–895.

Lamy, J., Lamy, J., & Weill, J. (1979c) *Arch. Biochem. Biophys. 193*, 140–149.

Lamy, J., Lamy, J., Sizaret, P.-Y., Billiald, P., Jolles, P., Jolles, J., Feldmann, R. J., & Bonaventura, J. (1984) *Biochemistry* (in press).

Long, C. (1961) *Biochemists Handbook*, Richard Clay and Co., Ltd., Bungay, Suffolk, England.

Markl, J., & Kempter, B. (1981) *J. Comp. Physiol. 141*, 495–502.

Markl, J., Savel, A., & Linzen, B. (1981) *Hoppe-Seyler's Z. Physiol. Chem. 362*, 1255–1262.

Marlborough, D. I. (1979) *Arch. Biochem. Biophys. 196*, 248–254.

Martell, A. E., & Smith, R. M. (1977) *Critical Stability Constants*, Plenum Press, New York.

Nickerson, K. W., & Van Holde, K. E. (1971) *Comp. Biochem. Physiol. B 39B*, 855–872.

Perrin, D. D., & Dempsey, B. (1974) *Buffers for pH and Metal Ion Control*, Halsted Press, New York.
Riggs, A. F., & Wolbach, R. A. (1956) *J. Gen. Physiol. 39*, 585-605.
Robertson, J. D. (1970) *Biol. Bull. (Woods Hole, Mass.) 138*, 157-183.
Roxby, R., Miller, K., Blair, D. P., & Van Holde, K. E. (1974) *Biochemistry 13*, 1662-1668.
Siezen, R. J., & Van Driel, R. (1973) *Biochim. Biophys. Acta 295*, 131-139.
Snyder, G. K., & Mangum, C. P. (1982) in *Physiology and Biology of Horseshoe Crabs* (Bonaventura, J., Bonaventura, C., & Tesh, S., Eds.) pp 173-188, Liss, New York.
Solomon, E. I., Eickman, N. C., Himmelwright, R. S., Hwang, Y. T., Plon, S. E., & Wilcox, D. E. (1982) in *Physiology and Biology of Horseshoe Crabs* (Bonaventura, J., Bonaventura, C., & Tesh, S., Eds.) pp 189-230, Liss, New York.
Sullivan, B., Bonaventura, J., & Bonaventura, C. (1974) *Proc. Natl. Acad. Sci. U.S.A. 71*, 2558-2562.
Svedberg, T., & Heyroth, F. F. (1929) *J. Am. Chem. Soc. 51*, 539-550.
Svedberg, T., & Hedenius, A. (1934) *Biol. Bull (Woods Hole, Mass.) 66*, 191-223.
van Bruggen, E. F. J., Bijlholt, M., Schutter, W., Wichertjes, T., Bonaventura, J., Bonaventura, C., Lamy, J., Lamy, J., Leclerc, M., Schneider, H., Markl, J., & Linzen, B. (1980) *FEBS Lett. 116*, 207-210.
Van Holde, K. E., & Brenowitz, M. (1981) *Biochemistry 20*, 5232-5239.

Purification of the Membrane-Spanning Tryptic Peptides of the α Polypeptide from Sodium and Potassium Ion Activated Adenosinetriphosphatase Labeled with 1-Tritiospiro[adamantane-4,3′-diazirine]†

Robert A. Nicholas

ABSTRACT: Five long, membrane-spanning tryptic peptides from the α polypeptide of sodium and potassium ion activated adenosinetriphosphatase [$(Na^+ + K^+)$-ATPase] have been purified. $(Na^+ + K^+)$-ATPase, isolated from canine kidney, was exposed to ultraviolet light in the presence of a high concentration of 1-tritiospiro[adamantane-4,3′-diazirine], a carbene precursor that partitions into the bilayer of the membrane. The α polypeptide, modified with 1.2 mol of [^{3}H]adamantylidene (mol of polypeptide)$^{-1}$, was isolated and digested with trypsin. Digestion with trypsin ensures that membrane-spanning sequences remain intact during the digestion, since lysine and arginine, being extremely hydrophilic, rarely appear in the membrane-embedded regions of membrane proteins. This digestion produced radioactive tryptic peptides greater than 25 residues in length. The tryptic digest of the labeled α polypeptide was chromatographed on Sephadex LH-60 in ethanol-formic acid, 4:1. The majority of the radioactivity (87%) eluted with distribution coefficients corresponding to peptides longer than melittin (26 residues), whereas 73% of the protein traveled with distribution coefficients corresponding to peptides less than 30 residues in length. Five radioactive peptides were further purified by high-pressure liquid chromatography, and each peptide displayed a unique, hydrophobic amino-terminal sequence. No other candidates could be found when a search for additional membrane-spanning peptides was conducted. Gel filtration of the tryptic peptides from the α polypeptide of $(Na^+ + K^+)$-ATPase labeled with 5-[^{125}I]iodo-1-naphthyl azide, a lipophilic nitrene precursor, produced no additional radioactive components. Amino-terminal sequences and amino acid compositions of the five purified peptides are presented.

Sodium and potassium ion activated adenosinetriphosphatase [$(Na^+ + K^+)$-ATPase][1] catalyzes the transport of three sodium ions out of the cell and two potassium ions into the cell, with the concomitant hydrolysis of MgATP (Skou, 1964). Purified preparations contain two components: a catalytic polypeptide of M_r 110000 ± 15000 designated α and a sialoglycoprotein of unknown function with a molecular weight of 55000 ± 10000 designated β (Craig & Kyte, 1980; Peterson & Hokin, 1981). The α polypeptide is known to span the membrane (Kyte, 1974) and contains the site of phosphorylation (Uesugi et al., 1971; Kyte, 1971a) and at least part of the binding site for cardiac glycosides (Ruoho & Kyte, 1974).

Since the homologous enzyme, calcium ion activated adenosinetriphosphatase (Ca^{2+}-ATPase), does not require a β polypeptide in order to function (MacLennan, 1970), the α

† From the Department of Chemistry, University of California, San Diego, La Jolla, California 92093. *Received August 2, 1983.* This research was supported by Grants GM-07619 and AM-07233 from the National Institutes of Health, Grant PCM78-24284 from the National Science Foundation, and Grant-in-Aid AHA81-1003 from the American Heart Association, all of which provide support to the laboratory of Jack Kyte.

[1] Abbreviations: $(Na^+ + K^+)$-ATPase, sodium and potassium ion activated adenosinetriphosphatase; Ca^{2+}-ATPase, calcium ion activated adenosinetriphosphatase; [^{3}H]adamantanediazirine, 1-tritiospiro-[adamantane-4,3′-diazirine]; HPLC, high-pressure liquid chromatography; $NaDodSO_4$, sodium dodecyl sulfate; TPCK-trypsin, trypsin treated by the manufacturer with L-1-(tosylamido)-2-phenylethyl chloromethyl ketone; CM-Cys, (carboxymethyl)cysteine; Tris, tris(hydroxymethyl)-aminomethane; EDTA, ethylenediaminetetraacetic acid.

0006-2960/84/0423-0888$01.50/0